Quantum processes and axion searches

Qiaoli Yang

based on arxiv 1912.11472 (to appear in PLB)
and arxiv 2201.08291
with Yu Gao & Zhihui Peng

Assuming QCD axions are one of the major components of DM

Axions produced during the QCD phase transition should be abundant

Axion fluctuations are correlated to the CMB fluctuation.

$$\langle \delta S_a^2 \rangle = \frac{2\sigma_\theta^2(2\theta_0^2 + \sigma_\theta^2)}{(\theta_0^2 + \sigma_\theta^2)^2}$$

- The observed CMB isocurvature fluctuation is small

$$\left\langle \left(\frac{\delta T}{T}\right)_{\rm iso}^2 \right\rangle \sim \langle \delta S_a^2 \rangle \lesssim \mathcal{O}(10^{-11}).$$

$$m_0 \approx 6 \times 10^{-5}\mathrm{eV}\left(\frac{10^{11}\mathrm{GeV}}{f_a}\right)$$

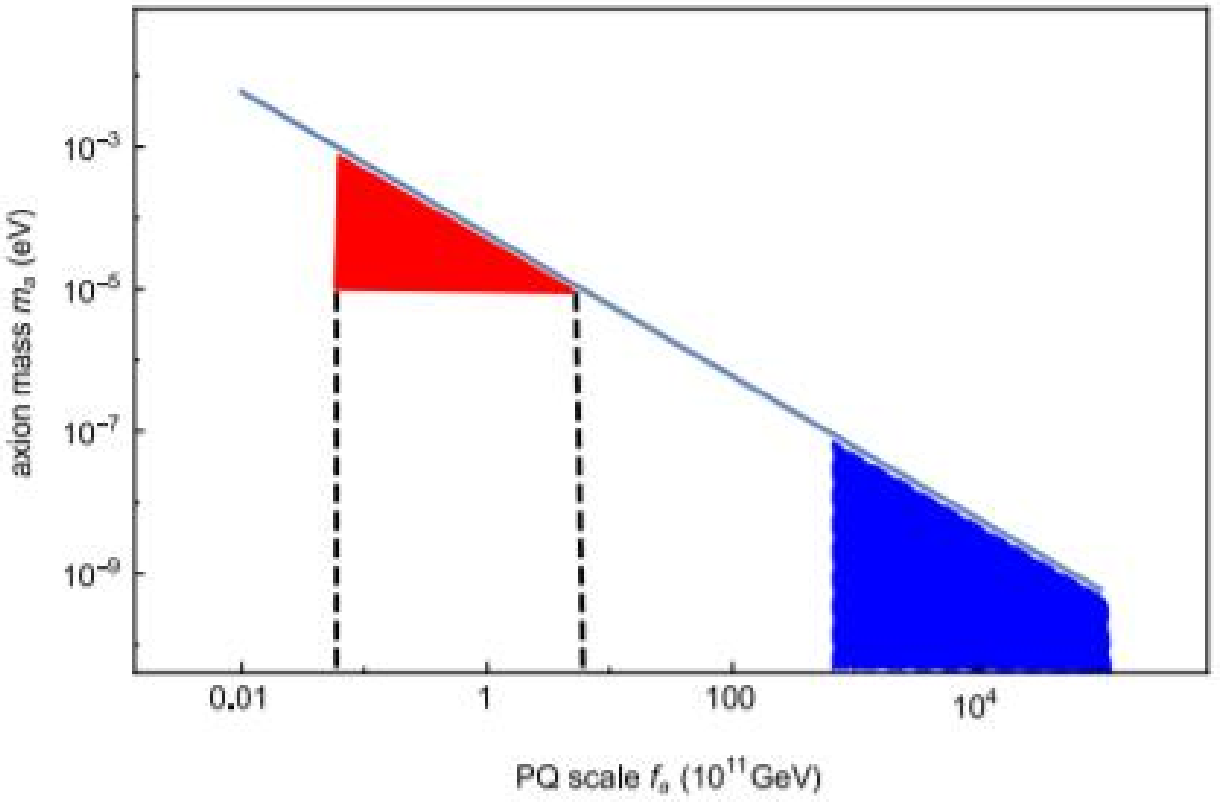

FIG. 1: The two possible windows of the dark matter axions. The upper-left one is often called the classical window and the lower-right one is the anthropic window assuming that $H_I < 10^{10}$GeV and the PQ symmetry was not restored after inflation.

Dark matter axions induce quantum transitions

$$a(x) \approx a_0 \cos(-m_a t - \frac{m_a}{2} v^2 t + m_a \vec{v} \cdot \vec{x} + \phi_0)$$

$$\bar{a}_0 \approx \sqrt{2\rho_{\mathrm{CDM}}}/m_a$$

The axion spectrum density I_a is high

$$I_a = \frac{\rho_{CDM}}{(1/2)m_a \delta v^2}$$

The interaction term in non-relativistic limit is:

$$H_{int} = \frac{1}{f_a} \sum g_f (\partial_t a \frac{\vec{p}_f \cdot \vec{\sigma}_f}{m_f} + \vec{\sigma}_f \cdot \vec{\nabla} a)$$

The transition rate is

$$R = \frac{\pi}{f_a^2} | \sum g_f < f | (\vec{v} \cdot \vec{\sigma}_f) | i > |^2 I_a$$

Hydrogen 1S state transitions

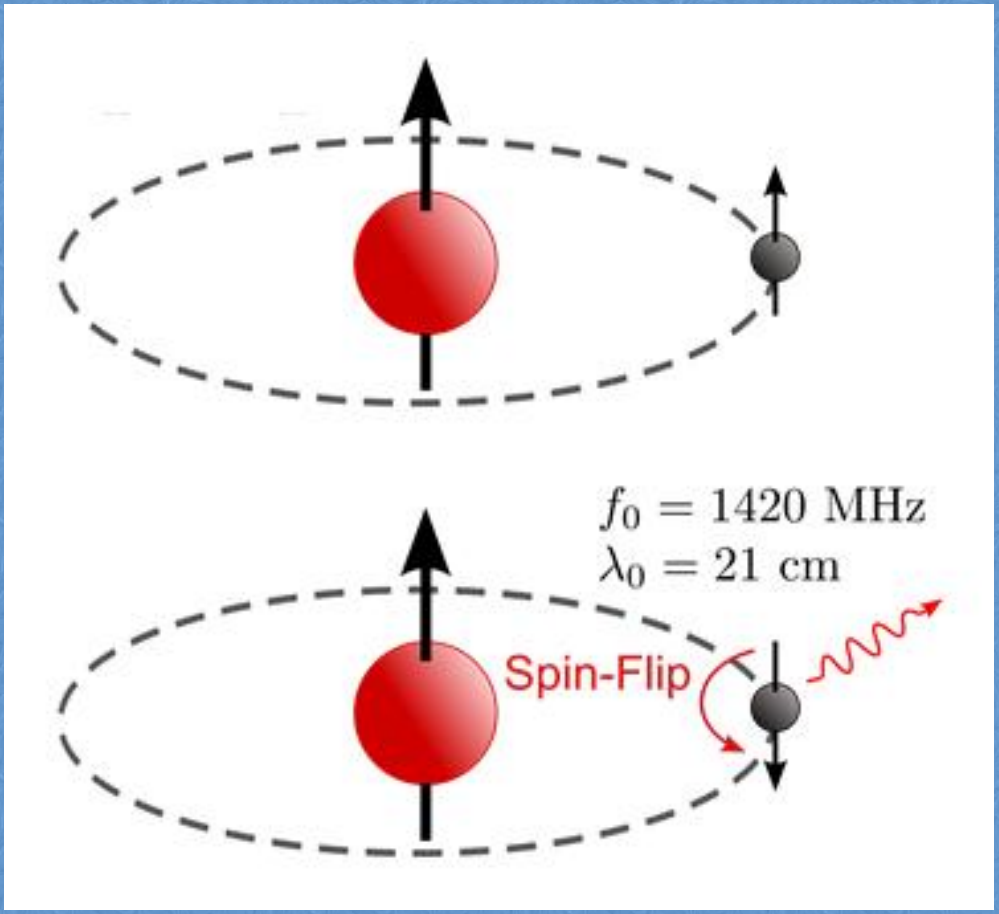

arxiv:1912.11472

Hydrogen atoms are ideal targets for the classical window

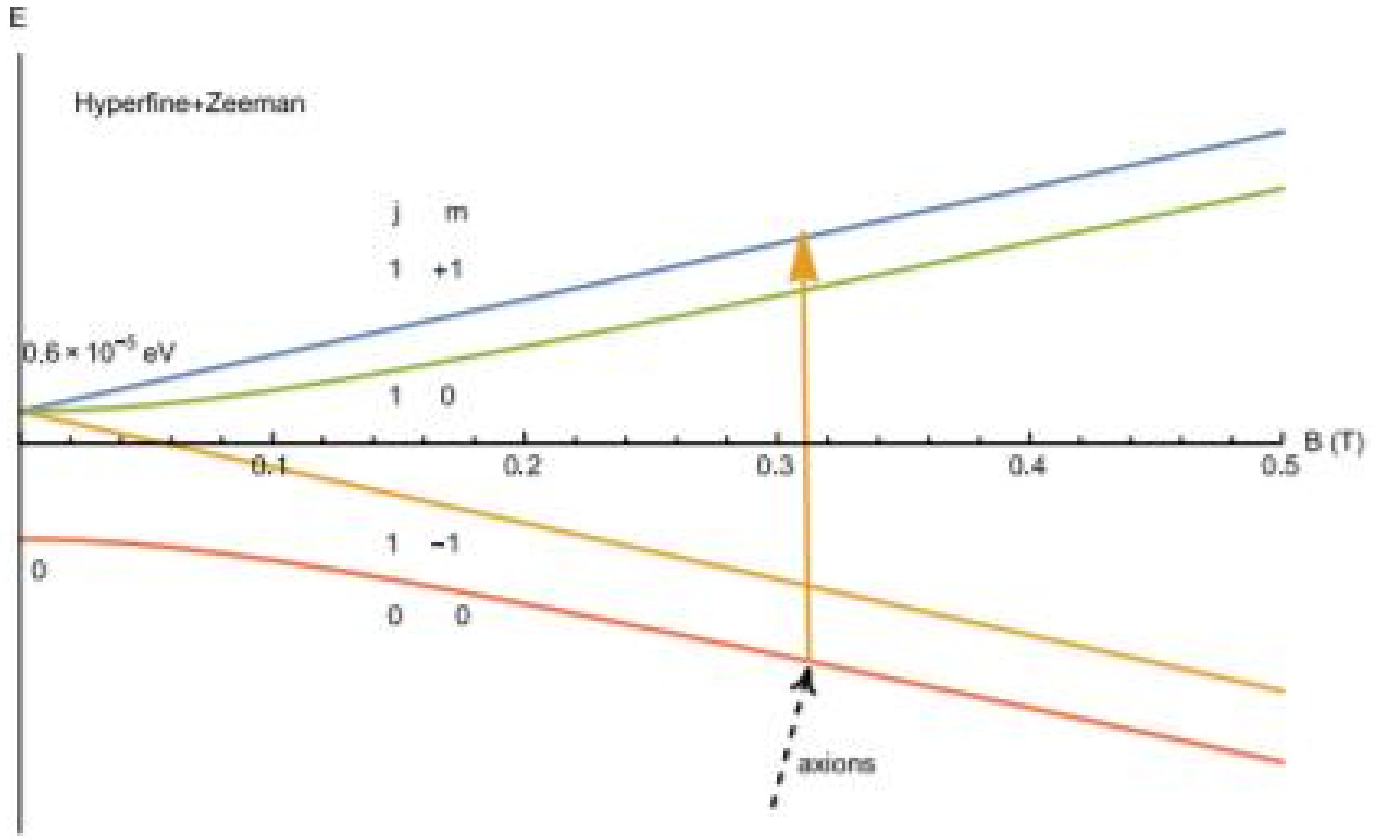

FIG. 2: The splitting of the hydrogen $1S$ state. For the classical window, $|0,0> \rightarrow |1,1>$ transition is suitable for the axion detection.

Hydrogen atoms are also ideal targets for the anthropic window

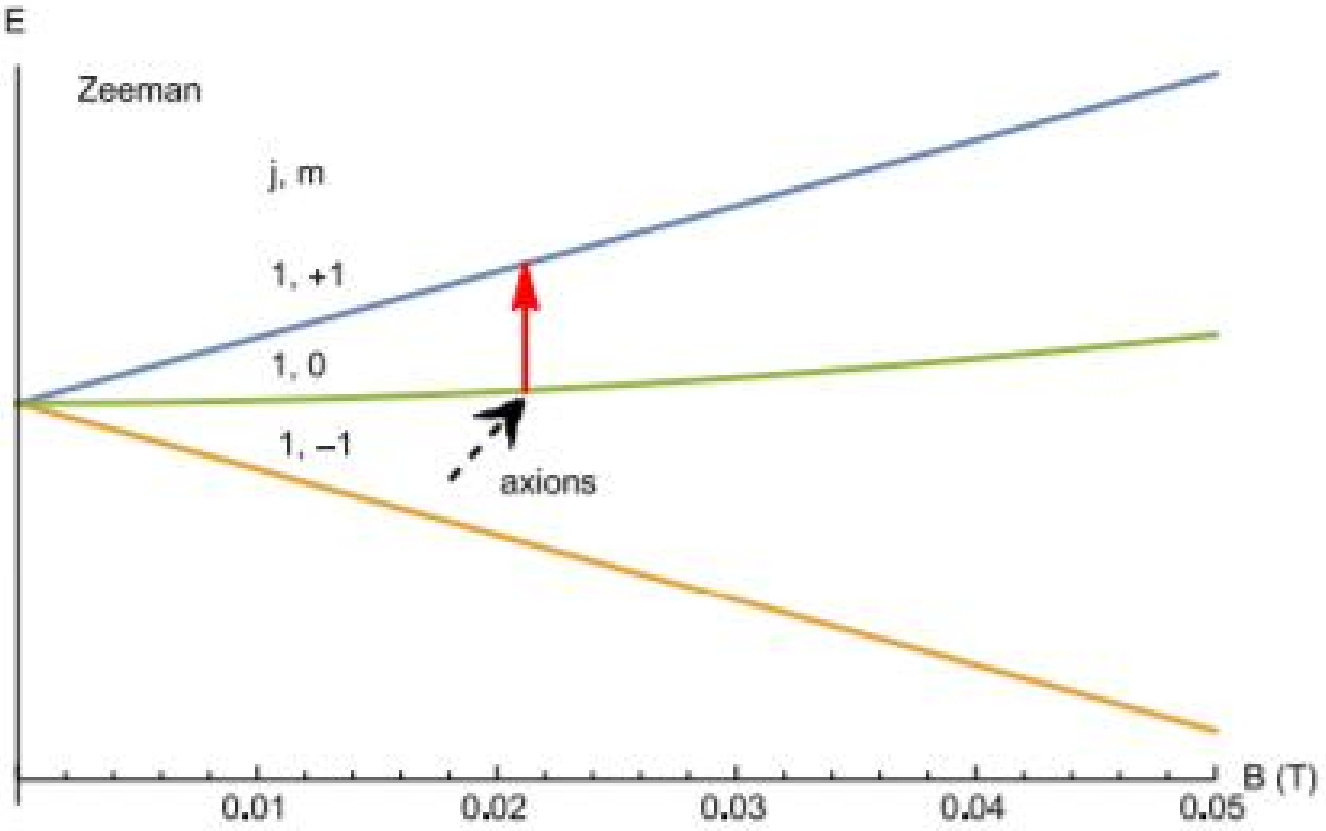

FIG. 3: The splitting of the hydrogen $1S$ triplet state. For the anthropic window $|1,0> \rightarrow |1,1>$ transition is suitable for the axion detection.

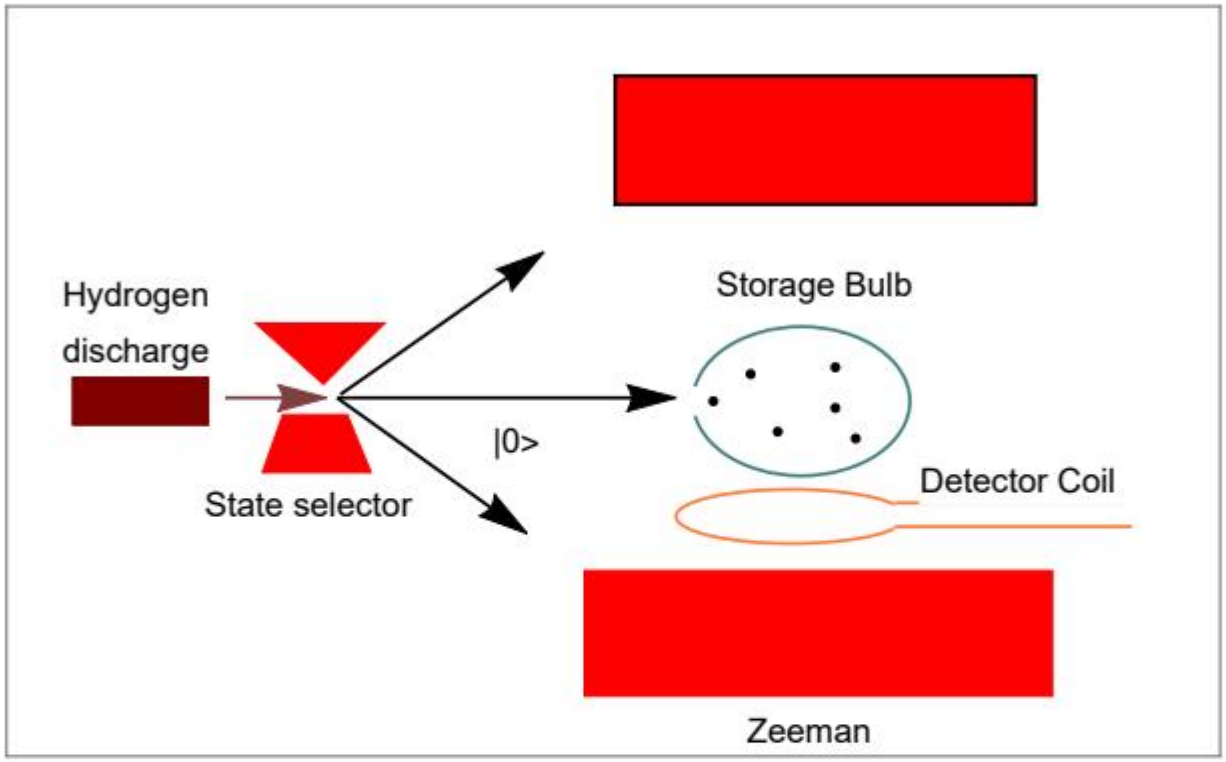

FIG. 4: Another possible setup of the proposed detection scheme which is similar to the hydrogen masers. The cold atoms go through a magnetic gate that allows only $m_j = 0$ states to pass. Subsequently, the atoms enter a storage bulb surrounded by a tunable Zeeman effect magnet. Once inside the bulb and the atomic energy gaps are matched with the axion mass. some atoms are resonantly excited to the $m_j = 1$ state, which is detectable by the magnetic field detector.

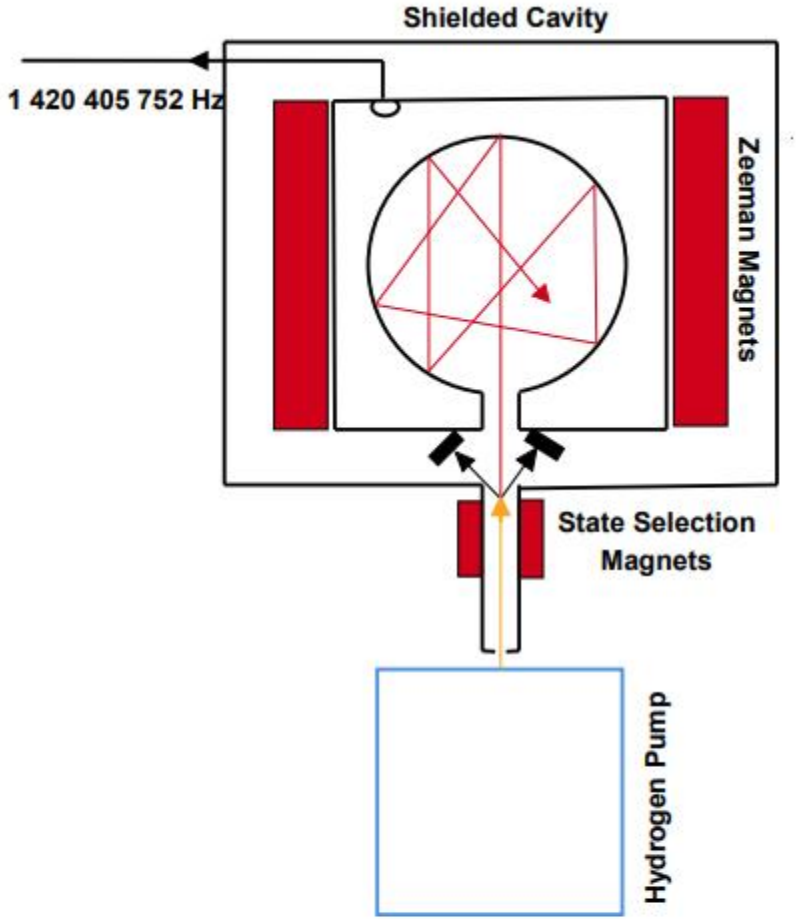

FIG. 5: An illustration of a typical hydrogen maser. With some modifications such as adding Zeeman magnets it may realize the scheme shown in Fig. 4.

The quantum properties of the Cavity

Modern cryogenic technology can sustain ~20mK or lower temperature

$$n(\omega_a, T) = \frac{1}{e^{\omega_a / k_B T} - 1}$$

The thermal photons have a very low occupation number n<<1 .

Thus it is useful to consider the quantum picture.

The Quantum picture of the Cavity (Feynman diagram method cannot be used here)

The axion photon coupling is

$$\mathcal{L}_{a\gamma\gamma} = -g_{a\gamma\gamma} a \vec{E} \cdot \vec{B}$$

The Quantum picture of the Cavity

The interaction Hamiltonian is

$$
\begin{aligned}
H_I &= -\int d^3x \mathcal{L}_{a\gamma\gamma} \\
&= \left(g_{a\gamma\gamma} \frac{\sqrt{2\rho_a}}{m_a} B_0 \int d^3x \hat{z} \cdot \vec{E} \right) \cos(\omega_a t)
\end{aligned}
$$

The Quantum picture of the Cavity

The electric field operator in the cavity can be expanded

$$\vec{E} = i\sum\sqrt{\frac{\omega_k}{2}}[a_k\vec{U}_k(\vec{r})e^{-i\omega_k t} - a_k^{\dagger}\vec{U}_k^{*}(\vec{r})e^{i\omega_k t}]$$

where $\vec{U}_k(\vec{r})$ is the cavity modes

The Quantum picture of the Cavity

The transition probability is

$$
\begin{aligned}
P &\approx \left| \langle 1 | \int_0^t dt H_I \, |0\rangle \right|^2 \\
&\approx g_{a\gamma\gamma}^2 \frac{\rho_a}{m_a^2} B_0^2 \sum_k \omega_k | \int d^3x \hat{z} \cdot \vec{U}_k^* |^2 \\
&\times \frac{\sin^2[(\omega_k - \omega_a)t/2]}{4[(\omega_k - \omega_a)/2]^2}
\end{aligned}
$$

The Quantum picture of the Cavity

The transition rate is

$$R \approx g_{a\gamma\gamma}^2 \frac{\rho_a}{m_a^2} B_0^2 V \sum_k C_k \omega_k \delta(\omega_k - \omega_a) \approx g_{a\gamma\gamma}^2 \frac{\rho_a}{m_a^2} B_0^2 C_{\omega_a} V Q$$

where

$$C_k = \frac{\left| \int d^3x \hat{z} \cdot \vec{U}_k \right|^2}{V \int d^3x |\vec{U}_k|^2}$$

The Quantum picture of the Cavity

The transition rate is enhanced by the cavity quality factor Q even for a single transition. Also, it is larger than the classical picture by a factor pi/2

Typical photon emitting rate of the cavity is order of 10Hz.

A cavity at quantum level can be regarded as a single photon emitter with a slow rate~ 10Hz.

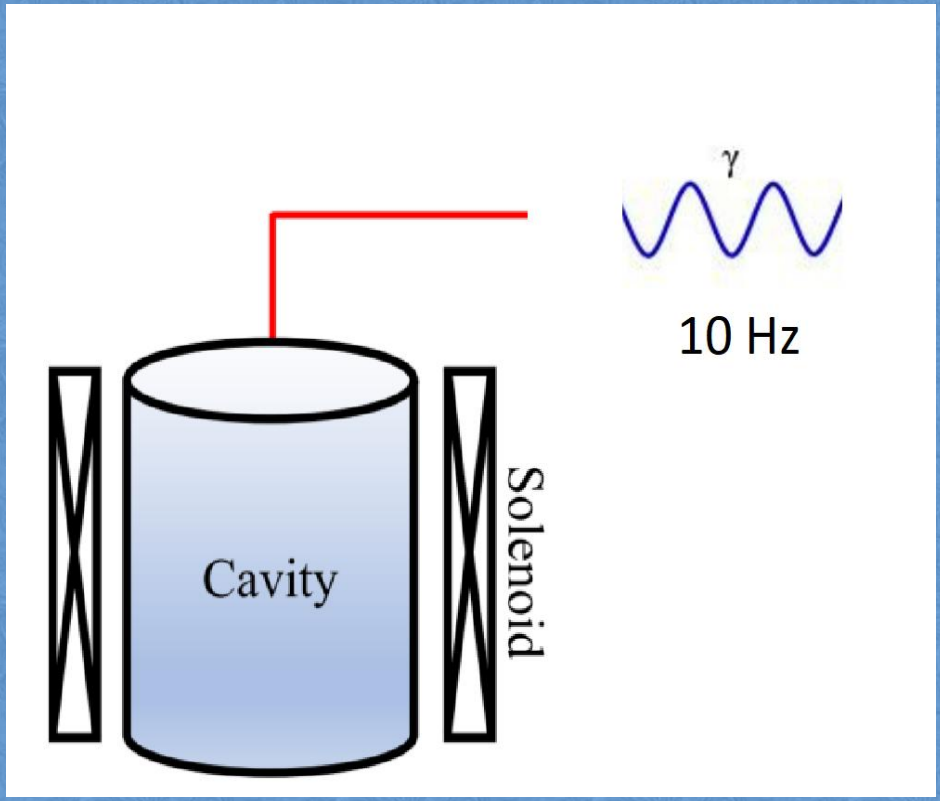

The bottleneck of the haloscope

The linear amplifier with a moderate bandwidth adds noise temperature order of T_eff=10K

$$\mathrm{SNR} = \frac{P_{sig}}{k_B T_{eff}} \sqrt{\frac{t}{b}}$$

The quantum interferometry

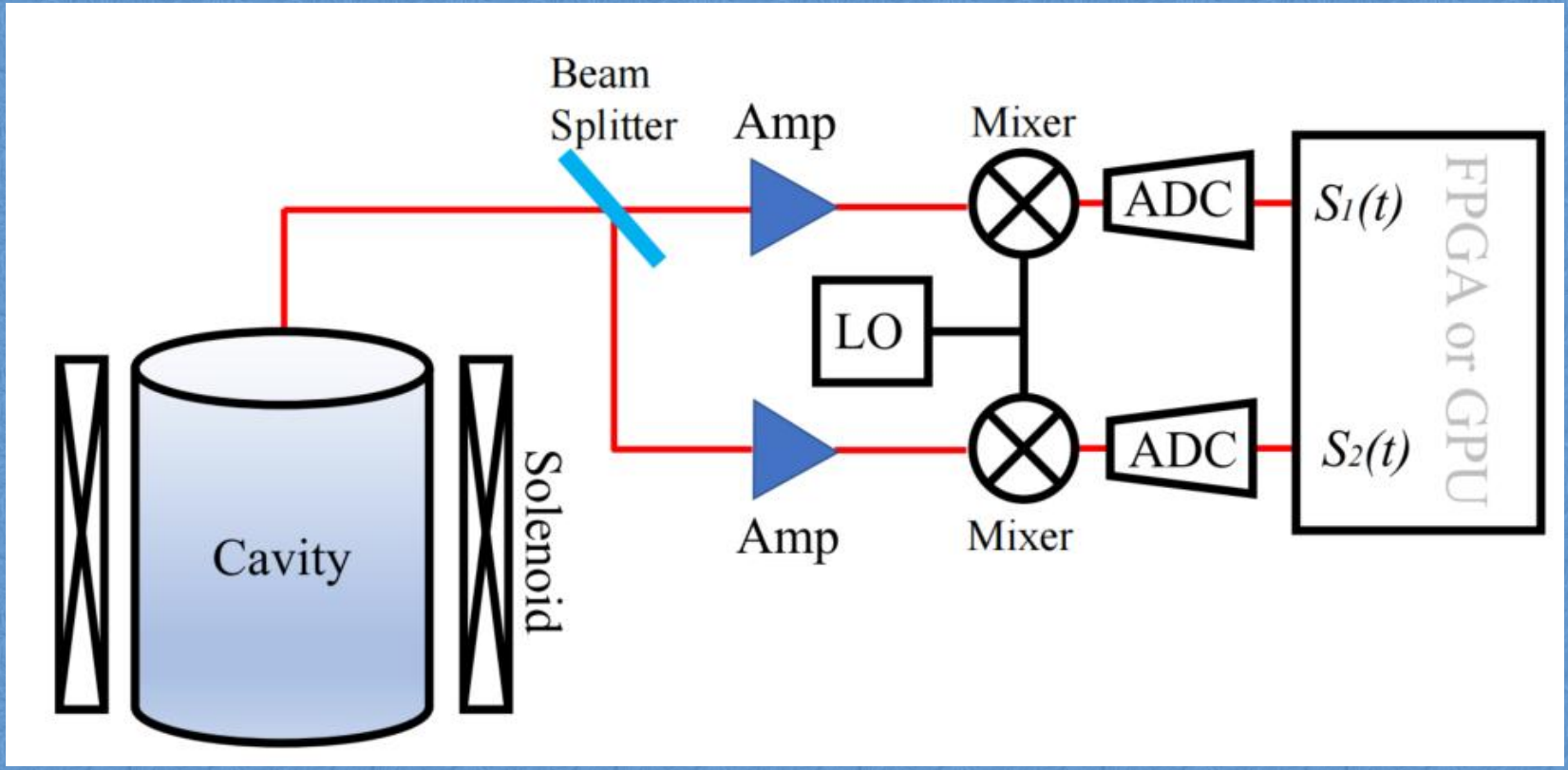

The quantum interferometry

The beam splitter gives two output fields in channel 1 and 2

$$\hat{r}_1 = (\hat{r} + \hat{\nu}_m)/\sqrt{2} \quad \text{and} \quad \hat{r}_2 = (\hat{r} - \hat{\nu}_m)/\sqrt{2}$$

$\hat{r}$ denotes the signal and $\hat{\nu}_m$ denotes the noises.

The quantum interferometry

Then one measures

$$\hat{I}_1 = (\hat{r}_1 + \hat{r}_1^+)/2$$

and

$$\hat{Q}_2 = -i(\hat{r}_2 - \hat{r}_2^+)/2$$

as the real and imaginary part of the field envelopes.

The quantum interferometry

The two path instantaneous power function is

$$\langle S_1^*(t) S_2(t) \rangle = G_1 G_2 \left(\langle \hat{r}^+(t) \hat{r}(t) \rangle + N_{12} \right)$$

where N_{12} is the power of correlated noise in channel 1 and 2

Simulated signal